ON THE PROBLEM OF RESOLUTION FOR FULLY COHERENT CSAS SYSTEM

Yan Pailhas[a], Yvan Petillot[a] & Bernard Mulgrew[b]

[a]Ocean Systems Lab, Heriot Watt University
[b]School of Engineering, University of Edinburgh

Riccarton Campus, EH14 4AS, Scotland, UK
email: Y.Pailhas@hw.ac.uk, www: https://researchportal.hw.ac.uk/en/persons/yan-pailhas/

Abstract: *ATR (Automatic Target Recognition) for MCM (MineCounter Measure) operations is highly dependent on resolution and image quality. The introduction of SAS (Synthetic Aperture Sonar) systems, more than a decade ago, has then been a game changer in the field of MCM. It became clear over the years however that single pass survey may not be sufficient to reach acceptable levels of recognition and/or false alarm. The interesting problem of target reacquisition has then emerged. For synthetic aperture systems, circular reacquisition patterns are particularly beneficial for various reasons: (i) it offers the full 360 degrees view angles of the target, (ii) it maximises the aperture offering the maximum theoretical resolution for the system and (iii) it is relatively efficient in term of reacquisition time. This presentation focuses on the resolution problem for CSAS systems. Thanks to the symmetry of the problem, we will derive the exact CSAS PSF (Point Spread Function) at the centre of the reacquisition pattern, then extend the exact PSF expression to the full field of view using atom wave wavelet analysis. We will naturally derive a new definition for resolution based on the PSF energy leakage. The PSF is not uniform for the full view area, and we will introduce two normalisation methods to remediate this issue. Finally, we will show how to increase further the CSAS resolution and then the image quality using pulse adapted wave atom deconvolution..*

Keywords: *CSAS, Resolution, Wave Atom Deconvolution.*

1. THE CSAS RESOLUTION

1.1. Configuration and nomenclature

We are considering a SAS system **S** performing a circle $\mathcal{C}$ centred in the point **O** and with a radius R. We define the full view area as the area where every point is *seen* by the SAS system **S** during its full trajectory on $\mathcal{C}$. Assuming that $\mathcal{C}$ is a circle, the full view area is then also a circle whose radius r is function of R and the beamwidth φ of the system:

$$r = R\sin(\varphi/2) \tag{1}$$

Figure 1 pictures the CSAS configuration described in this paper. The CSAS full view area is highlighted in blue in the figure.

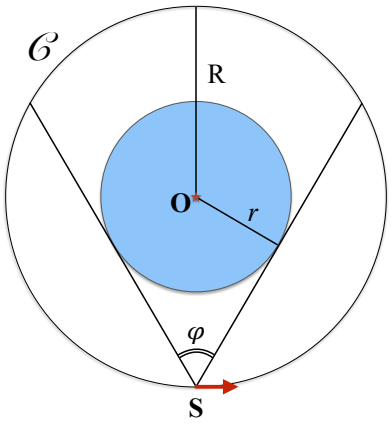

Fig. 1: Circular SAS configuration: **S** *location of the SAS system following the circular trajectory* $\mathcal{C}$ *centred in* **O**. *The CSAS full view area is highlighted.*

For the rest of the paper, we will be using the nomenclature described in Table 1 for the central frequency, the bandwidth, the pulse length and the Gaussian window temporal length related to the pulse. For the numerical simulations and unless otherwise specified, we will be using the values also indicated in Table 1.

Notations	Definition	Values	Units
c	sound speed	1500	$\mathrm{m.s}^{-1}$
f_0	pulse centre frequency	100	kHz
Δf	bandwidth	20	kHz
T	pulse length	1	ms
σ	Gaussian window temporal width	200	µs

Table 1: Nomenclature and nominal values.

1.2. The matched filter response

In this section, we compute the matched filter response of a linear frequency modulated (LFM) signal weighted by a rectangular window and a Gaussian window. The matched filter

response solves the range compression problem and plays an important role in the derivation of the PSF.

Let $p(t)$ be the pulse sent by the SAS system. We assume that $p(t)$ is a weighted LFM signal. Thus, we can write:

$$p(t) = W(t)\exp\left[2i\pi\left(f_0 + \frac{\Delta f}{2T}t\right)t\right], \tag{2}$$

where $W(t)$ is the windowing function. We are considering two cases for $W(t)$, a rectangular window:

$$W(t) = \mathbb{1}_{[-T/2,T/2]}(t), \tag{3}$$

and a Gaussian window:

$$W(t) = \exp\left(-\frac{t^2}{2\sigma^2}\right). \tag{4}$$

The matched filter response $s_{\mathrm{MF}}(t)$ of the pulse (2) is given by:

$$\begin{aligned} p_{\mathrm{MF}}(t) &= \int_{-\infty}^{+\infty} p^*(t')p(t'+t)\,\mathrm{d}t' \\ &= e^{2i\pi\left(f_0+\frac{\Delta f}{2T}t\right)t}\int_{-\infty}^{+\infty} W(t')W(t'+t)\exp\left[2i\pi\frac{\Delta f}{T}t't\right]\,\mathrm{d}t' \end{aligned} \tag{5}$$

The exact analytic expression of the matched filter response (5) can be found for both windowing functions (3) and (4) as described in [1] and [2] respectively, and $p_{\mathrm{MF}}(t)$ reduces to

$$p_{\mathrm{MF}}(t) = B(t)\,e^{2i\pi f_0 t}, \tag{6}$$

with

$$B(t) = T\frac{\sin[\pi t\Delta f(1-|t|/T)]}{\pi t\Delta f} \quad \text{for the rectangular windowing (3) and} \tag{7}$$

$$= \sigma\sqrt{\pi}\exp\left[-\left(\frac{1}{4\sigma^2}+\pi^2\frac{\Delta f^2}{T^2}\sigma^2\right)t^2\right] \quad \text{for the Gaussian windowing (4).} \tag{8}$$

For the Gaussian windowing case, $B(t)$ can be rewritten as $B(t) = \sigma\sqrt{\pi}\exp\left[-\frac{c^2}{8a_0^2}t^2\right]$ where $a_0 = \frac{1}{\sqrt{2}}\frac{c\sigma T}{\sqrt{T^2+4\pi^2\Delta f^2\sigma^4}}$ represents the spatial standard deviation.

Figures 2(a) and (b) plot the matched filter response of the pulse $p(t)$ for respectively the rectangular windowing (3) and the Gaussian windowing (4) with the pulse parameters described in Table 1. Note that the analytical formula (6) is exact and that there is a perfect match between the predicted and the simulated data.

From (6), it is interesting to note that the matched filter response $p_{\mathrm{MF}}(t)$ is only a low frequency envelope, $B(t)$, modulated by the central frequency f_0. The frequency content of $p_{\mathrm{MF}}(t)$ then comes from the frequency leakage caused by the windowing function $B(t)$.

1.3. CSAS Point Spread Function

To recover the CSAS PSF, we need to integrate the received echoes along the full circular trajectory $\mathcal{C}$. We consider an ideal scatterer located at the centre **O** of the circle $\mathcal{C}$. Given the

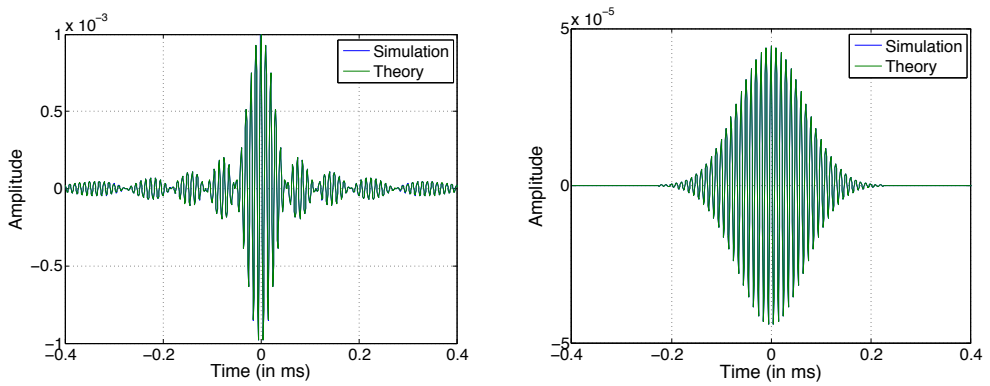

(a) (b)

Fig. 2: Match filtered response for a pulse with (a) rectangular window and (b) Gaussian window.

circular geometry of the problem, it is convenient to compute the PSF is the polar coordinates where **O** represents the origin. Furthermore, the PSF $I(r,\theta)$ is only function of r, the distance to the centre **O**, *i.e.* $I(r,\theta) = I(r)$. The integration along $\mathcal{C}$ gives the PSF, and we can write

$$I(r) = \int_{\theta=0}^{2\pi} B\left(\frac{2r\cos\theta}{c}\right) e^{4i\pi f_0 r\cos\theta/c}\, \mathrm{d}\theta. \tag{9}$$

Using a first order approximation of the MacLaurin series for $B(.)$ leads to the PSF expression for CSAS configuration:

$$I(r) = 2\pi B\left(\frac{2r}{c}\right) J_0(2kr) \tag{10}$$

with $k = 2\pi f_0/c$ representing the wave number and $J_0(.)$ the Bessel function of the first kind of order 0.

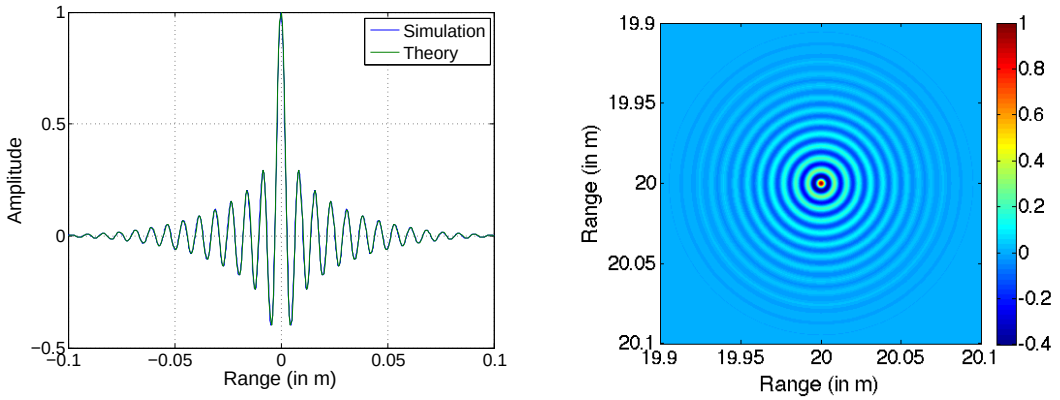

(a) (b)

Fig. 3: (a) Comparison between the full SAS integration from Eq. (9) *and the approximation from Eq.* (10) *for a pulse with a Gaussian windowing. (b) Normalised PSF for a CSAS system using a pulse with a Gaussian window.*

In figure 3(a), we plot the PSF as a function of r and compare the exact solution (9) with the approximation given by (10). The numerical simulation has been performed using the

numerical value given in Table 1. The close match between the two curves indicates that the first order approximation reflects accurately the circular integration. Figure 3(b) draws the 2D normalised CSAS PSF for a pulse with a Gaussian windowing.

2. DISCUSSION

The resolution argument plays an important role in the capability for a system to perform recognition tasks and in particular for automated target recognition algorithms [2–5]. Few points are worth highlighting from the results of section 1.

Resolution definition: The classic definition of resolution comes from the pulse compression technique as developed in section 1.2. For a linear frequency modulated (LFM) pulse, the distance resolution Δr is often defined as the -3dB spatial width of the matched filter response and is given by the classic formula:

$$\Delta r = \frac{c}{2\Delta f}. \tag{11}$$

First it is worth mentioning that the approximate formula (11) assumes a rectangular windowing function as written in (3) and then does not take into account any variation in the pulse shape or windowing. Eq. (11) often conjures up the -3dB spatial width as a definition. Again, this argument is approximate, the $\frac{c}{2\Delta f}$ represents in reality a -2.18dB spatial width, but $\frac{c}{2\Delta f}$ is in fact closer to half of the spacing between the first zeros of the $\mathrm{sinc}(.)$ function in (7). In [2] we propose to redefine the resolution as a percentage of the energy leaking of the PSF (Point Spread Function). This definition takes into account the specific pulse sent by the system and also infers on the degree of interference that a scatterer will have on adjacent pixels. As an example, the PSF radial energy E integrated over a radius r_0 of the the PSF for a fully coherent CSAS system given a LFM pulse with a Gaussian windowing can be written as:

$$E(r_0) = E_0 \,\mathrm{erf}(a_0 r_0) \tag{12}$$

where $E_0 = \pi^{3/2}\sigma^2 \frac{a_0}{2k}$ represents the total PSF energy. The radius r_0 pixel that integrates 90% of the PSF is then found by solving the equation: $\mathrm{erf}(a_0 r_0) = 90\%$.

Effective bandwidth: Bandwidth is not a quantity well defined nor easily measured for real system as it depends on the physical characteristics of the transducers and also the transmitted pulse itself. It is well known that rectangular windowing, although it maximises the overall pulse energy, creates Gibbs oscillations in the Fourier domain [6] and, as a result, strong oscillations in the matched filter response as seen in figure 3(a). Windowing functions, such as Gaussian, Hamming or Tukey, smooth these oscillations and provide much cleared response in the Fourier domain. The unfortunate consequence is a reduction in the bandwidth. We define the effective bandwidth as the bandwidth of a rectangular windowed pulse that would provide the same resolution of the tested transmitted pulse using the resolution definition described by (11). A Gaussian windowed LFM pulse for example has an effective bandwidth Δf_{eq} of

$$\Delta f_{\mathrm{eq}} = \frac{c}{4\sqrt{2\ln 1.65}a_0}. \tag{13}$$

The Gaussian windowed pulse with the parameters of Table 1 for example has an effective bandwidth of approximately 9kHz compared to the nominal 20kHz.

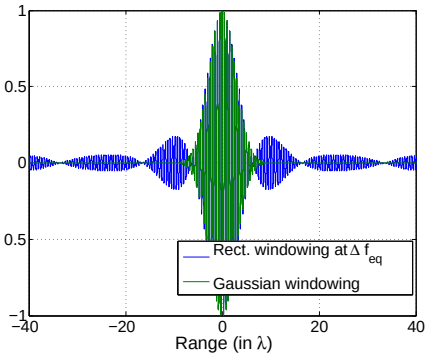

Fig. 4: Matched filter response of a Gaussian windowed LFM pulse and comparison with a rectangular windowed LFW pulse at Δf_{eq}.

CSAS resolution gain: As stated earlier, the principle of a CSAS strategy for target acquisition is to maximise the virtual antenna aperture length. With 2π integration, full coherent CSAS simply provides the maximum aperture possible. In essence, Eq. (10) describes the gain in resolution of the CSAS processing compared to the matched filter response alone. The resolution gain factor can be found by the asymptotic expression of the Bessel function $J_0(.)$ and writes as $\sqrt{\frac{2}{2\pi kr}}$. It is important to note that, contrary to the matched filter response, the CSAS processing gain is function of the central frequency f_0: as the central frequency increases, the resolution also increases. As seen in figure 5 and for a system operating at $f_0 = 100$kHz and described in Table 1, the gain in resolution is approximatively 16.

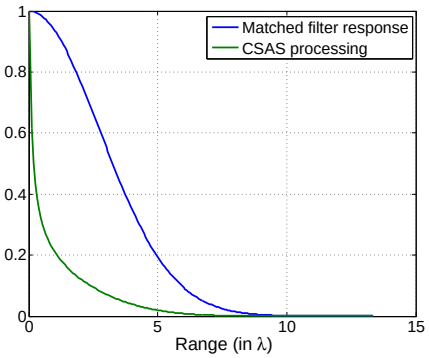

Fig. 5: CSAS processing resolution gain compared to matched filter processing alone.

ACKNOWLEDGEMENT

This work was supported by the Engineering and Physical Sciences Research Council (EPSRC) Grant number EP/J015180/1 and the MOD University Defence Research Collaboration in Signal Processing.

REFERENCES

[1] M. Cheney and B. Borden. *Fundamentals of Radar Imaging*. pp. 149. Society for Industrial and Applied Mathematics, Philadelphia, US, 2008.

[2] Y. Pailhas, Y. Petillot, and B. Mulgrew. Increasing circular synthetic aperture sonar resolution via adapted wave atoms deconvolution. *J. Acoust. Soc. Am.*, 141(4):2623–2632, 2017.

[3] Yan Pailhas, Yvan Petillot, Chris Capus, and Keith Brown. Real-time sidescan simulator and applications. In *OCEANS 2009-EUROPE*, pages 1–6. IEEE, 2009.

[4] Y. Pailhas, Y. Petillot, and C. Capus. High-resolution sonars: What resolution do we need for target recognition? *EURASIP Journal on Advances in Signal Processing*, 2010(1):205095, 2010.

[5] Y. Pailhas, Y. Petillot, K. Brown, and B. Mulgrew. Spatially distributed mimo sonar systems: Principles and capabilities. *IEEE Journal of Oceanic Engineering*, 42(3):738–751, July 2017.

[6] J. W. Gibbs. Fourier's Series. *Nature*, 59, 1898.